Proc. Natl. Acad. Sci. USA
Vol. 93, pp. 2941–2946, April 1996
Biochemistry

Mutagenesis by third-strand-directed psoralen adducts in repair-deficient human cells: High frequency and altered spectrum in a xeroderma pigmentosum variant

(triplex/gene targeting/supF/shuttle vector/DNA repair)

MANIDIPA RAHA*, GAN WANG*, MICHAEL M. SEIDMAN†, AND PETER M. GLAZER*‡

*Department of Therapeutic Radiology, Yale University School of Medicine, P.O. Box 208040, New Haven, CT 06520-8040; and †OncorPharm, 200 Perry Parkway, Gaithersburg, MD 20877

Communicated by Alan Garen, Yale University, New Haven, CT, November 1, 1995

ABSTRACT **Psoralen-conjugated triple-helix-forming oligonucleotides have been used to generate site-specific mutations within mammalian cells. To investigate factors influencing the efficiency of oligonucleotide-mediated gene targeting, the processing of third-strand-directed psoralen adducts was compared in normal and repair-deficient human cells. An unusually high mutation frequency and an altered mutation pattern were seen in xeroderma pigmentosum variant (XPV) cells compared with normal, xeroderma pigmentosum group A (XPA), and Fanconi anemia cells. In XPV, targeted mutations were produced in the *supF* reporter gene carried in a simian virus 40 vector at a frequency of 30%, 3-fold above that in normal or Fanconi anemia cells and 6-fold above that in XPA. The mutations generated by targeted psoralen crosslinks and monoadducts in the XPV cells formed a pattern distinct from that in the other three cell lines, with mutations occurring not just at the damaged site but also at adjacent base pairs. Hence, the XPV cells may have an abnormality in trans-lesion bypass synthesis during repair and/or replication, implicating a DNA polymerase or an accessory factor as a basis of the defect in XPV. These results may help to elucidate the repair deficiency in XPV, and they raise the possibility that genetic manipulation via triplex-targeted mutagenesis may be enhanced by modulation of the XPV-associated activity in normal cells.**

Oligonucleotides can bind to duplex DNA and form triple helices in a sequence-specific manner (1–4). Progress in elucidating the third-strand binding code has led to efforts to exploit nucleic acids as sequence-specific DNA binding reagents for research and possibly therapeutic applications (5). Oligonucleotide-mediated triplex formation has been shown to prevent transcription factor binding to promoter sites and to block mRNA synthesis *in vitro* and *in vivo* (for review, see ref. 5). It has also been used in strategies to create unique cleavage sites in DNA *in vitro* (6). We have explored the use of triplex-forming oligonucleotides as a mechanism to deliver a tethered mutagen to a selected gene for the site-specific introduction of DNA damage (7–10). Psoralen-conjugated oligonucleotides directed to a site in a mutation reporter gene were found to induce targeted mutations in λ and simian virus 40 (SV40) DNA in experiments in which the triplex formation was carried out *in vitro* (7, 8). In recent work, conditions were determined under which targeted mutagenesis of an SV40 vector could be achieved *in vivo* in monkey COS cells via intracellular triplex formation using psoralen-linked triplex-forming oligonucleotides (10), demonstrating the potential utility of modified oligonucleotides for *in vivo* genetic manipulation.

The publication costs of this article were defrayed in part by page charge payment. This article must therefore be hereby marked "*advertisement*" in accordance with 18 U.S.C. §1734 solely to indicate this fact.

Successful gene targeting by this approach depends not only on efficient triplex formation and damage induction but also on the processing of the targeted damage in the cell via repair or replication into the desired genetic change. To uncover relevant processing pathways, we investigated mutagenesis by targeted psoralen photoadducts in a series of human repair-deficient cell lines, including xeroderma pigmentosum complementation group A (XPA), xeroderma pigmentosum variant (XPV), and Fanconi anemia (FA).

These cell lines were chosen for analysis because they form a diverse collection of repair deficiencies. XPA cells have a defect in a DNA damage recognition and binding protein that is a component of a ternary repair endonuclease complex in nucleotide excision repair (11, 12). The defect in XPV cells is less well characterized, but inferences from several sets of experiments (13–17) have led to the suggestion that XPV cells have an abnormality in DNA synthesis at sites of damage. FA cells have been found to be particularly sensitive to DNA crosslinking agents, including psoralen (18), and may be prone to deletions via a mechanism associated with abnormal variable–diversity–joining (VDJ) recombination (19).

We report the observation of an unusually high frequency of targeted mutations in the XPV cells (an average of 30%), along with a unique spectrum of mutations distinct from that seen in XPA, FA, or normal cell lines. We propose mechanisms to explain these findings, and we suggest that these results not only may help to characterize the DNA repair defect in XPV cells but also may lead to novel strategies to enhance the third-strand-mediated genetic manipulation of mammalian cells.

MATERIALS AND METHODS

Oligonucleotides. Psoralen-linked oligonucleotides were prepared as described (7–10). The psoralen is incorporated into the oligonucleotide synthesis as a psoralen phosphoramidite, resulting in an oligonucleotide linked at its 5′ end via a two-carbon linker arm to 4′-hydroxymethyl-4,5′,8-trimethylpsoralen, pso-AGGAAGGGGG (pso-AG10). Pso-S-S-AG10, containing a disulfide bond in the linker arm connecting the psoralen to the oligonucleotide, was synthesized by incorporation of a thiol modifier (S–S) phosphoramidite (Glen Research, Sterling, VA) into the automated synthesis prior to the addition of the 5′ psoralen. To preserve the disulfide linker in the synthesis, modification of the oxidation step was required, as directed by Glen Research.

Vectors. Construction of the shuttle vector plasmid pSP189 has been described (20).

Abbreviations: XPA, xeroderma pigmentosum, group A; XPV, xeroderma pigmentosum variant; FA, Fanconi anemia; UVA, long-wavelength UV light; UVC, short-wavelength UV light; DTT, dithiothreitol; SV40, simian virus 40.

‡To whom reprint requests should be addressed.

Cells. Human cell lines were obtained from the NIGMS Human Genetic Mutant Cell Repository (Camden, NJ). XPA cells (repository designation GM04429E) are SV40-transformed fibroblasts derived from a patient with XPA (XP12BE). XPV cells (GM02359) are primary fibroblasts derived from a patient with the XPV (XP115LO). FA cells (GM06914B) are SV40-transformed fibroblasts obtained from a patient with FA (1309VA). Normal fibroblasts (GM00637F) are SV40-transformed cells derived from an apparently normal donor. The cells were grown in MEM-E supplemented with 10% (vol/vol) fetal calf serum (GIBCO/BRL).

Targeted Photoadduct Formation. In a reaction volume of 10 μl, 3 μg (50 nM) of the pSP189 DNA was incubated with a 100:1 molar excess of either pso-AG10 or pso-S–S-AG10 (0.3 μg, 5 μM) for 2 h at 37°C in 10% (wt/vol) sucrose/20 mM $MgCl_2$/10 mM Tris·HCl, pH 8.0/1 mM spermidine. Irradiation of samples with either long-wavelength UV light (UVA; 1.8 J/cm^2) or visible light (12 J/cm^2) was performed as described (7–10).

In the case of pso-S–S-AG10, the irradiated mixture was further incubated with 50 mM dithiothreitol (DTT) at 55°C for 4 h to release the oligonucleotide by disulfide bond reduction. The detached oligonucleotide was separated from the modified duplex by heating the mixture at 65°C for 5 min and filtration through a Centricon-100 filter (Amicon), yielding pSP189 DNA containing a site-specific psoralen adduct without an associated oligonucleotide.

Successful detachment of the oligonucleotide from the targeted psoralen adduct was monitored by end-labeling pso-S–S-AG10 with dideoxyadenosine 5′-[α-^{32}P]triphosphate using terminaltransferase. The pSP189 and labeled pso-S–S-AG10 complex was analyzed before and after DTT treatment and Centricon-100 filtration by alkaline agarose gel electrophoresis and autoradiography.

Transfection. The cells were transfected with the plasmid DNAs, either unmodified or containing third-strand-targeted psoralen adducts, premixed with cationic liposomes (Lipofectamine, GIBCO/BRL) following the manufacturer's protocol. Approximately 3 μg of plasmid DNA were used per 5 × 10^5 cells.

Shuttle Vector Isolation and Analysis. Shuttle vector DNA was isolated from the cells and used to transform bacteria for *supF* gene analysis as described (7–10).

DNA Sequencing. Sequencing of the *supF* genes in the mutant colonies was performed as described (10), using a primer chosen to bind to the β-lactamase gene just upstream of the *supF* gene in the vector (20).

Statistics. The mutation spectra were compared pairwise by using the two-tailed Fischer's exact test. In the case of UVA photoactivation, the mutations were scored as either occurring at position 167 or not at position 167. In the analysis of the visible light-induced spectra, the mutations were scored as at position 166 or not at position 166.

RESULTS

Experimental Strategy. Third-strand-targeted mutagenesis in human cells was studied by using an SV40-based shuttle vector, pSP189 (7, 20). This vector contains the *supF* gene, an amber suppressor tyrosine tRNA gene of *Escherichia coli*, serving as a mutation reporter, along with both the SV40 and pBR327 origins of replication. A 10-base oligonucleotide conjugated to a psoralen derivative at its 5′ end, psoralen-AGGAAGGGGG (pso-AG10), was designed to bind as a third strand to bp 167–176 of the *supF* gene in the purine antiparallel triplex motif (7, 8, 21) and to thereby position the psoralen for intercalation and adduct formation at the 5′ ApT 3′ site at bp 166 and 167. The third-strand binding site is indicated within the *supF* sequence in Fig. 1.

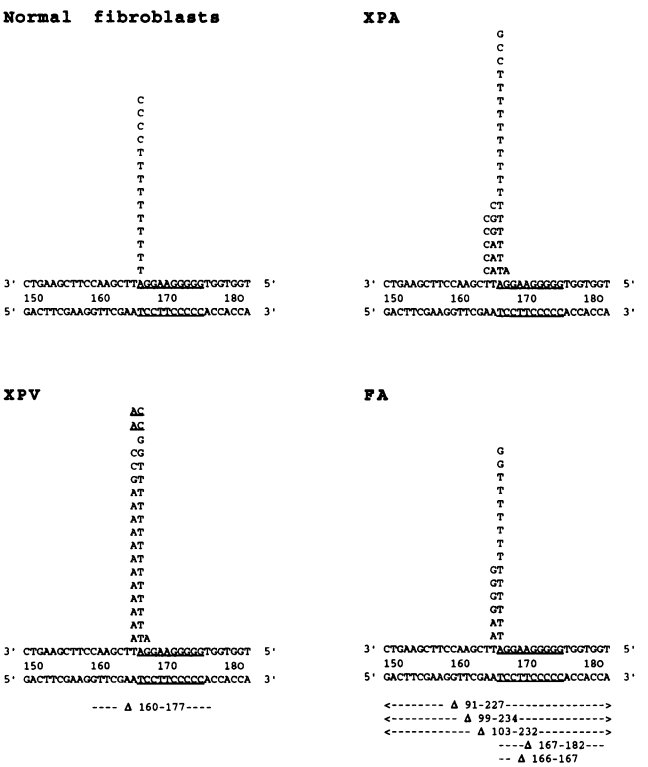

FIG. 1. Spectra of *supF* gene mutations produced in normal and repair-deficient human cells by UVA-activated third-strand-targeted psoralen adducts. Point mutations are indicated above each base pair, with the listed base representing a change from the sequence in the top strand. The underlined point mutations represent simultaneous tandem base changes; otherwise, all indicated point mutations were single base pair changes. Deletion mutations are presented below the *supF* sequence, indicated by the dashed lines. The underlined nucleotides in the *supF* sequence delineate the third-strand binding site.

After triplex formation, targeted psoralen adducts are generated by either UVA or visible light photoactivation (7–10). Upon UVA irradiation (1.8 J/cm^2), 65% of the plasmid DNAs have a psoralen interstrand crosslink between the thymidines in bp 166–167, 20% have a psoralen monoadduct at the thymidine in bp 166, 10% have a monoadduct at the thymidine in bp 167, and 5% are not covalently modified (9). With visible light photoactivation (12 J/cm^2 of 447 nm light), 40% of the plasmid DNAs have a monoadduct on the thymidine in bp 166, while no more than 1% have a monoadduct on the thymidine at bp 167 and no more than 1% have a crosslink between the thymidines at bp 166 and 167. Fifty-eight percent of the plasmid DNAs remain unmodified.

The vector DNA carrying the premutagenic psoralen adducts is transfected into selected human cells in culture. Mutations in the *supF* gene are produced via repair and/or replication and are detected upon shuttle vector rescue into bacteria (7–10).

Mutagenesis in Repair-Deficient Cells. This protocol was used to test mutagenesis by targeted psoralen adducts in several human cell lines, including fibroblasts derived from patients with XPA, XPV, and FA, as well as from an apparently normal donor (Table 1). With pso-AG10 plus UVA treatment of the pSP189 DNA, the frequency of mutations observed in vectors rescued from the normal fibroblasts was found to be 11.5%. In contrast, only 5.7% of the vectors rescued from the XPA cells were mutated. This difference suggests that, in the normal cells, at least some of the targeted mutations arise in the process of excision repair, which is essentially absent in the XPA cells. FA cells showed a frequency similar to that seen in the normal cells. However, XPV

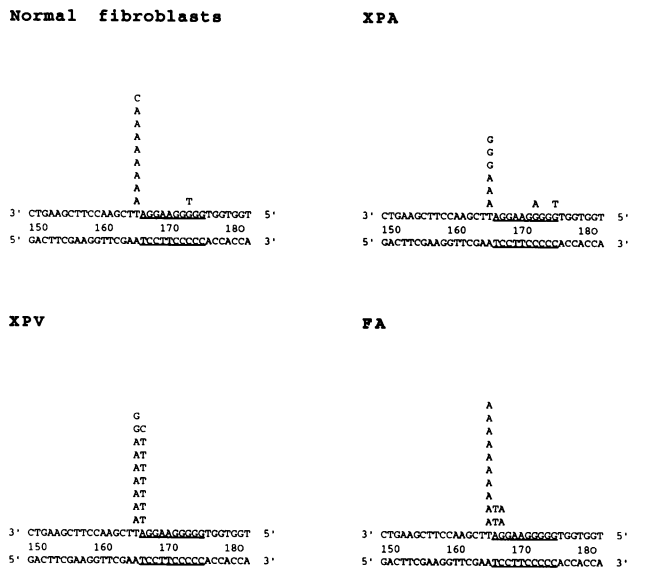

FIG. 2. Spectra of *supF* gene mutations produced in normal and repair-deficient human cells by visible-light-activated third-strand-targeted psoralen monoadducts. Mutations are listed as in Fig. 1.

cells yielded a surprisingly high frequency of targeted mutations; 30.5% of the vectors isolated from the XPV cells had mutations in the *supF* gene.

Mutation Spectra. The sequences of the mutations generated in the four cell lines were determined (Fig. 1). Similar spectra of mutations were seen in the normal fibroblasts, the XPA cells, and the FA cells. In these cell lines, most of the mutations occurred at bp 167, and the majority were T → A to A → T transversions. No mutations at position 166 were seen in the normal cells, and only 19% of the mutations from XPA cells and 23% of those from FA cells were at bp 166. In contrast, in the XPV cells, almost as many mutations were found at bp 166 as at bp 167. The mutation spectra in the normal fibroblasts and in the XPV cells were significantly different ($P = 0.002$), whereas those in the normal, XPA, and FA cells were not ($P > 0.05$ in all pairwise comparisons).

Table 1. Mutagenesis induced by third-strand-targeted psoralen adducts in human repair-proficient and repair-deficient cell lines

Cell line	Vector treatment†	No. mutants/ no. total	Mutation frequency, %
Normal fibroblast	None	3/15,000	0.02
	pso-AG10 + visible light	720/42,000	1.7
	pso-AG10 + UVA	700/6,100	11.5
XPA	None	7/35,000	0.02
	pso-AG10 + visible light	348/42,000	0.8
	pso-AG10 + UVA	349/6,100	5.7
XPV	None	5/11,000	0.05
	pso-AG10 + visible light	300/30,000	1.0
	pso-AG10 + UVA	3,350/11,000	30.5
FA	None	10/18,000	0.06
	pso-AG10 + visible light	684/28,000	2.4
	pso-AG10 + UVA	1,300/13,000	10.0

For vector treatment, after triple-helix formation by pso-AG10, the vector-psoralen-oligonucleotide complex was irradiated with either 1.8 J/cm^2 of UVA (365 nm) or 12 J/cm^2 of visible light (447 nm), as indicated. Control samples included untreated vector (None) that was neither irradiated nor incubated with the oligonucleotide. The values for the number of mutants represent the frequency of *supF* mutations detected in the pSP189 SV40-based shuttle vector after liposome-mediated transfection of the vector-psoralen-oligonucleotide DNA into the indicated cells and rescue of the vectors for genetic analysis of the *supF* gene in bacteria 48 h later.

Mutagenesis by Targeted Monoadducts. When the cells were transfected with targeted psoralen monoadducts, the mutation frequency was in the range of 1–2% for all the cell lines tested (Table 1). The lower mutation frequencies reflect, in part, the reduced efficiency of photoproduct formation upon visible light photoactivation. However, after normalizing for the degree of photoadduct formation and for the mixture of monoadducts and crosslinks after UVA irradiation, the data suggest that crosslinks are 4-fold more mutagenic than monoadducts in normal cells and 20-fold more mutagenic in the XPV cells.

In the XPV cells, the pattern of monoadduct-induced mutations was again distinct (Fig. 2). Most of the mutations in the normal, XPA, and FA cells were found at bp 166, consistent with the fact that almost all of the visible light-induced adducts are produced at this position. However, in the XPV cells, only 53% of the mutations occurred at bp 166, while 47% occurred at bp 167. Again, the differences between XPV and the other cells were statistically significant ($P = 0.02$), whereas there were no significant differences between the normal cells and either the XPA or the FA cell lines.

Mutagenesis by Targeted Adducts Detached from the Third Strand. Interpretation of this data is potentially complicated by the fact that the psoralen adduct is presented to the cell in the context of the triple helix. We therefore developed a strategy to direct psoralen adducts to the selected site in the *supF* gene in such a way that we could subsequently detach and separate the oligonucleotide from the psoralen moiety. An oligonucleotide with the same sequence as pso-AG10 was synthesized to contain a disulfide bond connecting the psoralen to the rest of the oligonucleotide, yielding pso-S–S-AG10 (Fig. 3*A*).

The same protocol for targeted adduct formation was used with the pso-S–S-AG10 oligomer. However, after photoactivation of the tethered psoralen the disulfide bond was reduced via DTT treatment to detach the oligonucleotide segment. The detached oligonucleotide was then removed by filtration above the triplex melting temperature. Detachment of the radioactively labeled oligonucleotide was documented by the analysis shown in Fig. 3*B*. The samples before and after DTT treatment are shown in lanes 2 and 3, respectively. To examine the specificity of the triplex-targeted photoreaction while at the same time verifying the release of the tethered oligonucleotide, the samples were digested with *Apa*LI. This generates two fragments of 4.4 and 0.6 kb, as shown by the ethidium bromide-stained sample of an *Apa*LI digest of the pSP189 plasmid DNA (lane 1). The triplex binding site is contained in the 0.6-kb fragment, which is visualized in lane 2 because of the specific attachment of the radiolabeled oligonucleotide to that fragment. Note that there is no detectable labeling of the 4.4-kb band, showing the specificity of the triplex targeting. After the DTT treatment (lane 3), it can be seen that the label has been removed from the 0.6-kb band, demonstrating detachment of the oligonucleotide.

The results of mutagenesis experiments using pso-S–S-AG10 are shown in Table 2. In comparison to experiments with pso-AG10 (Table 1), lower induced mutation frequencies were seen in all the cell lines. These lower frequencies likely reflect a lower absolute efficiency of covalent psoralen adduct formation using pso-S–S-AG10 as opposed to pso-AG10, as determined by gel mobility shift assays under denaturing conditions (approximately 3.5-fold fewer adducts upon UVA irradiation, data not shown). Nonetheless, the targeted psoralen adducts still generated an elevated mutation frequency in the XPV cells. Hence, the XPV cells have an abnormality in the processing of psoralen-damaged DNA whether or not the psoralen adducts occur in the context of an associated third strand.

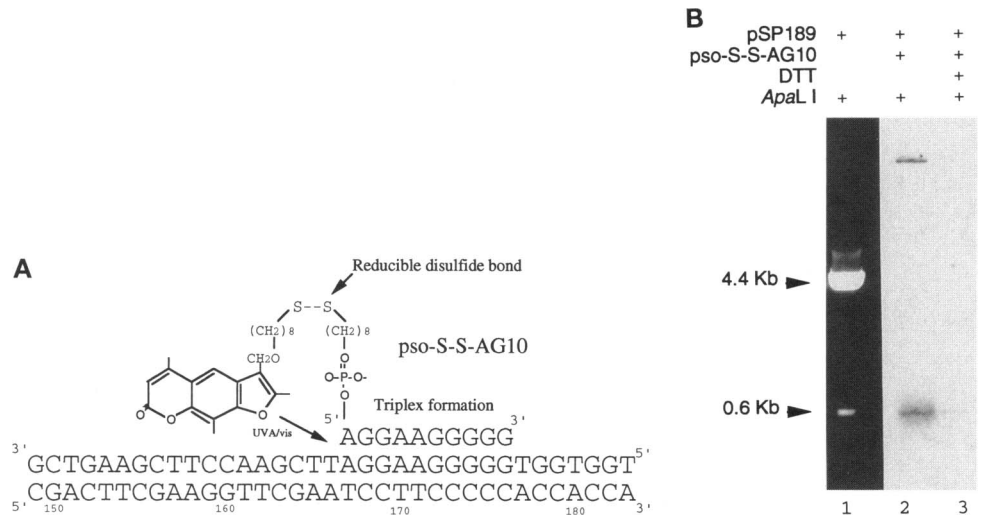

FIG. 3. Psoralen adduct targeting by a detachable triplex-forming oligonucleotide. (*A*) Structure of pso-S–S-AG10, a psoralen-conjugated oligonucleotide containing a disulfide linker between the oligonucleotide and the psoralen, designed to deliver and then separate from site-specific psoralen adducts at bp 166–167 within the *supF* gene, as indicated. (*B*) Visualization of psoralen adduct targeting by pso-S–S-AG10 and the subsequent detachment of the oligonucleotide. The SV40 shuttle vector pSP189 was incubated as indicated with pso-S–S-AG10 radiolabeled at the 3′ end. After UVA photoactivation to generate psoralen adducts, one sample was treated with DTT and then digested with *Apa*LI (lane 3), while another was digested with *Apa*LI without DTT treatment (lane 2). The products were analyzed by alkaline agarose gel electrophoresis and autoradiography to visualize the presence or absence of the oligonucleotide on the 0.6-kb fragment containing the triplex target site. In parallel, a sample of pSP189 DNA digested with *Apa*LI was visualized by ethidium bromide staining instead of autoradiography to show both the 4.4- and 0.6-kb digestion products (lane 1), as indicated. Note that the upper band in lane 2 represents material that did not enter the gel.

Sequence analysis of the pso-S–S-AG10-targeted mutations (Fig. 4) revealed that, in the normal cells, the pattern was the same as in the case of pso-AG10 (Figs. 1 and 2), with mutations mostly at bp 166 after visible light photoactivation and at bp 167 after UVA. In the XPV cells, the patterns were again different, with mutations occurring at both bp 166 and 167 after either visible light or UVA. With visible light, some mutations in XPV were also seen at bp 165. To explain these mutations, we considered the possibility that the longer linker arm connecting the psoralen to the TFO in pso-S–S-AG10 (Fig. 3*A*) might allow the tethered psoralen to reach the thymidine in bp 165 and form photoadducts at that site. This was confirmed using a DNA polymerase chain termination assay (data not shown).

DISCUSSION

In this work, we have studied mutagenesis by third-strand-directed psoralen adducts in normal and repair-deficient human cells. We have observed that XPV cells are uniquely defective in the processing of both monoadducts and crosslinks, resulting in elevated mutation frequencies and altered mutation spectra compared to normal, XPA, and FA cells.

Table 2. Psoralen adduct mutagenesis targeted by a detachable triplex-forming oligonucleotide

Cell line	Irradiation	No. mutants/ no. total	Mutation frequency, %
Normal fibroblast	Visible light	2,200/280,000	0.8
	UVA	8,000/125,000	6.4
XPA	Visible light	500/130,000	0.4
	UVA	4,000/102,500	3.9
XPV	Visible light	3,000/450,000	0.7
	UVA	32,000/320,000	10.0
FA	Visible light	1,600/320,000	0.5
	UVA	16,000/260,000	6.2

After triple-helix formation by pso-S–S-AG10, the vector-psoralen-oligonucleotide complex was irradiated as for Table 1. The samples were then incubated with DTT to reduce the disulfide bond and detach the psoralen adduct from the tethered oligonucleotide, which was removed by filtration. Values for mutation frequency were determined as for Table 1.

XPV Defect. Previous studies of XPV cells have revealed hypermutability but approximately normal cell survival after short-wavelength UV light (UVC) irradiation (16, 17, 22) and almost normal levels of nucleotide excision repair (13, 23). Other work has shown diminished DNA synthesis and strand elongation after UVC treatment (13–15), as well as inefficient psoralen adduct removal (24). Recent studies have shown that XPV cells are prone to misincorporation opposite UVC-damaged templates (16, 17) and exhibit altered UVC mutation hotspots (22).

Consistent with these reports, we have observed an unusual mutation spectrum in XPV. However, because we have used site-directed psoralen adducts, we can make the additional observation that XPV cells are prone to misincorporation not just at the precise position of the adduct but also at adjacent sites.

Mutagenesis by Monoadducts. In the normal, XPA, and FA cells, targeted monoadducts at bp 166 led to primarily T·A → A·T transversions at that position (Fig. 3). Since monoadduct repair should be relatively error-free (and is absent in the XPA cells), these mutations likely arise via translesion bypass synthesis during replication, causing misincorporation of a thymidine opposite the damaged thymidine in the template at bp 166.

In the XPV cells, however, mutations were generated at both bp 166 and 167. Considering the polarity of the strands and the consequent direction of DNA synthesis across the adduct on the thymidine in bp 166, position 167 represents the base pair that comes after the site of damage. Errors at this site may arise from template dislocation and slippage (25), which could be associated with an abnormality in polymerase proofreading and/or processivity during replication, due either to a polymerase mutation or to a defect in an accessory factor, such as proliferating cell nuclear antigen or replication protein A (26).

Mutagenesis by Crosslinks. In XPV, the crosslinks resulted in mutations at both bp 166 and 167, while in the other lines, the mutations were mostly at bp 167 (Fig. 2). We propose that

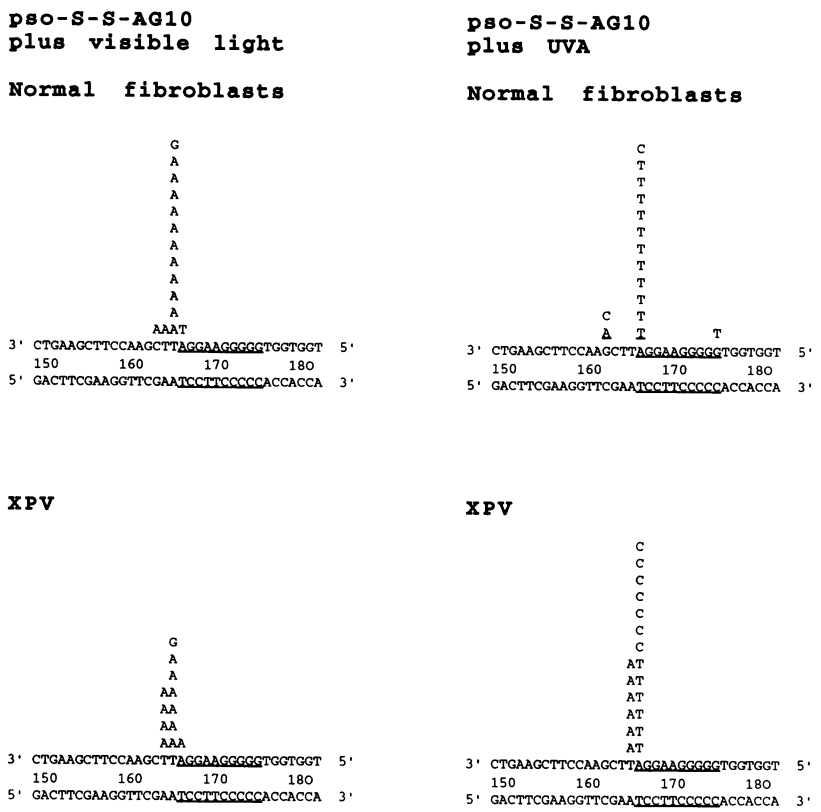

FIG. 4. Spectra of *supF* gene mutations produced in normal and XPV cells by third-strand-targeted psoralen adducts detached from the targeting oligonucleotide. Mutations are listed as in Figs. 2 and 3.

these mutations occur in the process of gap-filling repair synthesis during nucleotide excision repair. In this pathway (27, 28), a multiprotein complex recognizes and excises the damage via dual incisions in the damaged strand 6 nt 3′ and 22 nt 5′ from the site of damage (29). Release of the damaged DNA fragment via helicase activity creates a gap that is filled by repair synthesis (27).

Complete repair of psoralen crosslinks may involve sequential excision repair acting on both damaged strands. The initial strand repaired is determined in part by the orientation of the psoralen crosslink, with the furan-side lesion preferentially repaired first (30). In the pso-AG10-directed crosslink, the furan-side adduct is predominantly on the thymidine at position 166, and so repair would, therefore, be biased toward the strand containing this thymidine (9). After excision of the damaged fragment from that strand, gap-filling repair synthesis would have to bypass the remaining lesion on the other strand at position 167, potentially leading to a mutation at that site. [A more detailed discussion of this model for psoralen adduct repair and mutagenesis in the context of a triple helix has been published elsewhere (31).]

We therefore suggest that the abnormal crosslink mutation pattern in XPV results from defective repair synthesis across the adduct at bp 167. This proposed defect is consistent with the report of Hansson *et al.* (23) that XPV cell extracts show a variable level of repair synthesis, possibly due to an unusually labile repair factor in these cells. Thus, the abnormalities in monoadduct and crosslink mutagenesis suggest that the XPV cells are defective in a factor common to both DNA repair and replication.

The abnormal mutation pattern in the XPV cells was produced by the targeted psoralen adducts both in the presence and in the absence of the triplex-forming oligonucleotide, as shown by the experiments in which the oligonucleotide was detached by disulfide bond reduction. Therefore, our results can be attributed to the targeted psoralen adducts and do not necessarily depend on the associated third strand. In addition, the strategy described here to generate targeted adducts that are detachable from the targeting oligonucleotide may have general utility in the study of DNA repair and mutagenesis as a convenient approach to the creation of DNA substrates with site-specific damage.

We also observed a 3-fold reduced survival of the psoralen-damaged vectors in the XPV cells (data not shown). This suggests further that the XPV cells have difficulty in the replicative bypass of DNA damage, leading not only to more mutations but also to diminished vector replication.

Implications for Gene Targeting. Overall, the results presented here suggest that there can be significant variability in the frequency of the third-strand-directed mutagenesis, depending on several factors. These include not only the efficiency of triplex formation and the ability to generate site-specific DNA damage, but also, to a large extent, the capacity of the target cell to repair and replicate the damaged DNA. Cells may differ with regard to some or all of these factors based on genetic differences, as shown by the present work, or they may vary because of other characteristics, such as tissue of origin.

The large differences in targeted mutation frequencies seen in this work also suggest that strategies aimed at manipulation of cellular repair and replication pathways may enhance the prospects of using triplex-targeted damage for genetic manipulation. Since targeted psoralen adducts are converted into mutations at such a high frequency in XPV cells, modulation of normal cells to reproduce the XPV defect or to temporarily alter the XPV-associated pathway could enhance oligonucleotide-mediated targeted mutagenesis. For example, treatment of cells with caffeine has been shown to increase the sensitivity of XPV cells to DNA damage (13), and this type of manipulation could be tested in conjunction with triplex-directed gene

targeting. However, full exploitation of this pathway may not be possible until the XPV gene is cloned and the defect is more fully characterized.

We thank F. P. Gasparro and A. F. Faruqi for helpful discussions and P. A. Havre, E. J. Gunther, T. Yeasky, R. Franklin, and S. J. Baserga for their assistance. This work was supported by grants to P.M.G. from the Charles E. Culpeper Foundation, the Leukemia Society of America, the American Cancer Society (CN128), the National Institutes of Health (ES05775 and CA64186), and by a grant to M.R. from the Yale Skin Disease Research Center (P30AR41942).

1. Letai, A. G., Palladino, M. A., Fromm, E., Rizzo, V. & Fresco, J. R. (1988) *Biochemistry* **27,** 9108–9112.
2. Moser, H. E. & Dervan, P. B. (1987) *Science* **238,** 645–650.
3. Praseuth, D., Perrouault, L., Le Doan, T., Chassignol, M., Thuong, N. & Helene, C. (1988) *Proc. Natl. Acad. Sci. USA* **85,** 1349–1353.
4. Cooney, M., Czernuszewicz, G., Postel, E. H., Flint, S. J. & Hogan, M. E. (1988) *Science* **241,** 456–459.
5. Helene, C. (1991) *Anti-Cancer Drug Design* **6,** 569–584.
6. Strobel, S. A., Doucette-Stamm, L. A., Riba, L., Housman, D. E. & Dervan, P. B. (1991) *Science* **254,** 1639–1642.
7. Havre, P. A. & Glazer, P. M. (1993) *J. Virol.* **67,** 7324–7331.
8. Havre, P. A., Gunther, E. J., Gasparro, F. P. & Glazer, P. M. (1993) *Proc. Natl. Acad. Sci. USA* **90,** 7879–7883.
9. Gasparro, F. P., Havre, P. A., Olack, G. A., Gunther, E. J. & Glazer, P. M. (1994) *Nucleic Acids Res.* **22,** 2845–2852.
10. Wang, G., Levy, D. D., Seidman, M. M. & Glazer, P. M. (1995) *Mol. Cell. Biol.* **15,** 1759–1768.
11. Jones, C. J. & Wood, R. D. (1993) *Biochemistry* **32,** 12096–12104.
12. Park, C. H. & Sancar, A. (1994) *Proc. Natl. Acad. Sci. USA* **91,** 5017–5021.
13. Lehman, A. R., Kirk-Bell, S., Arlett, C. F., Paterson, M. C., Lohman, P. H., de Weerd-Kastelein, E. A. & Bootsma, D. (1975) *Proc. Natl. Acad. Sci. USA* **72,** 219–223.
14. Boyer, J. C., Kaufmann, W. K., Brylawski, B. P. & Cordeiro-Stone, M. (1990) *Cancer Res.* **50,** 2593–2598.
15. Griffiths, T. D. & Ling, S. Y. (1991) *Mutagenesis* **6,** 247–251.
16. Wang, Y. C., Maher, V. M. & McCormick, J. J. (1991) *Proc. Natl. Acad. Sci. USA* **88,** 7810–7814.
17. Wang, Y. C., Maher, V. M., Mitchell, D. L. & McCormick, J. J. (1993) *Mol. Cell. Biol.* **13,** 4276–4283.
18. Diatloff-Zito, C., Papadopoulo, D., Averbeck, D. & Moustacchi, E. (1986) *Proc. Natl. Acad. Sci. USA* **83,** 7034–7038.
19. Laquerbe, A., Moustacchi, E., Fuscoe, J. C. & Papadopoulo, D. (1995) *Proc. Natl. Acad. Sci. USA* **92,** 831–835.
20. Parris, C. N. & Seidman, M. M. (1992) *Gene* **117,** 1–5.
21. Beal, P. A. & Dervan, P. B. (1991) *Science* **251,** 1360–1363.
22. Waters, H. L., Seetharam, S., Seidman, M. M. & Kraemer, K. H. (1993) *J. Invest. Derm.* **101,** 744–748.
23. Hansson, J., Keyse, S. M., Lindahl, T. & Wood, R. D. (1991) *Cancer Res.* **51,** 3384–3390.
24. Misra, R. R. & Vos, J. M. (1993) *Mole. Cell. Biol.* **13,** 1002–1012.
25. Kunkel, T. A. (1990) *Biochemistry* **29,** 8003–8011.
26. Shivji, K. K., Kenny, M. K. & Wood, R. D. (1992) *Cell* **69,** 367–374.
27. Sancar, A. & Tang, M. S. (1993) *Photochem. Photobiol.* **57,** 905–921.
28. Wood, R. D., Aboussekhra, A., Biggerstaff, M., Jones, C. J., O'Donovan, A., Shivji, M. K. & Szymkowski, D. E. (1993) *Cold Spring Harbor Symp. Quant. Biol.* **58,** 625–632.
29. Huang, J. C., Svoboda, D. L., Reardon, J. T. & Sancar, A. (1992) *Proc. Natl. Acad. Sci. USA* **89,** 3664–3668.
30. Wood, R. D. (1985) *J. Mol. Biol.* **184,** 577–585.
31. Wang, G. & Glazer, P. M. (1995) *J. Biol. Chem.* **270,** 22595–22601.